

where Ni(II) complexes of the fluorinated cyclams were used as electrocatalysts for CO₂ reduction to CO in H₂O, suggests a promising application of fluorinated cyclams in redox-involving cyclam chemistry.^{28b,c,30}

(30) (a) Jubran, N.; Cohen, H.; Koresh, Y.; Meyerstein, D. *J. Chem. Soc., Chem. Commun.* **1984**, 1683. (b) Blake, A. J.; Gould, R. O.; Hyde, T. I.; Schröder, M. *J. Chem. Soc., Chem. Commun.* **1987**, 431.

Acknowledgment. The present study was supported by a Grant-in-Aid for Scientific Research, 01771933 (to M.S.), from the Ministry of Education, Science and Culture.

Supplementary Material Available: Listing of anisotropic thermal parameters (1 page); table of calculated and observed structure factors (5 pages). Ordering information is given on any current masthead page.

Synthesis, X-ray Structure, and Spectroscopic and Electrochemical Properties of Novel Heteronuclear Ruthenium–Osmium Complexes with an Asymmetric Triazolate Bridge

Ronald Hage,^{1a} Jaap G. Haasnoot,^{*1a} Heleen A. Nieuwenhuis,^{1a} Jan Reedijk,^{1a} Dirk J. A. De Ridder,^{1b} and Johannes G. Vos^{*1c}

Contribution from the Department of Chemistry, Gorlaeus Laboratories, Leiden University, P.O. Box 9502, 2300 RA Leiden, The Netherlands, Laboratory of Crystallography, University of Amsterdam, Nieuwe Achtergracht 166, 1018 WV Amsterdam, The Netherlands, and School of Chemical Sciences, Dublin City University, Dublin 9, Ireland. Received May 9, 1990

Abstract: The heterodinuclear compounds [(bpy)₂Ru(bpt)Os(bpy)₂](PF₆)₃ (RuOs) and [(bpy)₂Os(bpt)Ru(bpy)₂](PF₆)₃ (OsRu), where Hbpt = 3,5-bis(pyridin-2-yl)-1,2,4-triazole and bpy = 2,2'-bipyridine, have been prepared and characterized. The crystal and molecular structures of [(Ru(bpy)₂)₂(bpt)](CF₃SO₃)₃·4H₂O and [(bpy)₂Ru(bpt)Os(bpy)₂](CF₃SO₃)₃·4H₂O have been determined. The dinuclear ruthenium(II) compound crystallizes in the monoclinic space group *P*2₁/*c* with four molecules in a cell of dimensions *a* = 13.510 (1) Å, *b* = 16.110 (2) Å, *c* = 29.861 (4) Å, β = 99.225 (9)°. Only one of the two possible geometrical isomers of the ruthenium dinuclear compound was found in the crystal structure. The two metal centers are coordinated via N(1) and N(4) of the triazole ring with a Ru(1)–N(1) distance of 2.03 (1) Å and a Ru(2)–N(4) distance of 2.11 (1) Å. The metal–metal distance is 6.184 (2) Å. In [(bpy)₂Ru(bpt)Os(bpy)₂](CF₃SO₃)₃·4H₂O with *Z* = 4, *P*2₁/*c*, *a* = 13.5802 (7) Å, *b* = 16.247 (2) Å, *c* = 30.043 (3) Å, β = 100.348 (6)°, ruthenium is coordinated via N(1), whereas osmium binds via N(4) of triazole with similar metal–nitrogen distances as observed for the ruthenium homonuclear compounds. The NMR data revealed that the OsRu isomer has a similar structure, but with the osmium center bound via N(1) and the ruthenium ion coordinated via N(4) of the triazole ring. The electrochemical potentials of the two heterodinuclear compounds are significantly different; for the RuOs compound the oxidation potentials are 0.73 and 1.20 V, while for the OsRu isomer the oxidation potentials are at 0.65 and 1.30 V vs SCE. These differences in electrochemical behavior between the two isomeric RuOs and OsRu compounds suggest that the N(1) atom of the triazole ring is a better σ-donor than N(4). The mixed-valence dinuclear systems all exhibit rather intense intervalence transition (IT) bands in the near-infrared region, suggesting a moderately strong metal–metal interaction for the bpt systems. A correlation between the energy of the IT bands of the mixed-valence dinuclear complexes and the oxidation potentials has been observed.

Introduction

[Ru(bpy)₃]²⁺ (bpy = 2,2'-bipyridine) and related complexes have been the subject of many investigations because of their varied photophysical and electrochemical properties.^{1–6} Also dinuclear ruthenium and osmium compounds have been the subject of much research, not only because of their possible application as two-

electron-transfer reagents in water splitting devices, but also because of the current interest in the properties of mixed-valence compounds,^{7–12} the theory of which has been developed in detail by Hush.¹³

(1) (a) Leiden University. (b) University of Amsterdam. (c) Dublin City University.

(2) Seddon, E. A.; Seddon, K. R. *The Chemistry of Ruthenium*; Elsevier Science Publisher BV: Amsterdam, 1984.

(3) (a) Meyer, T. J. *Acc. Chem. Res.* **1978**, *11*, 94. (b) Meyer, T. J. *Pure Appl. Chem.* **1986**, *58* (9), 1193.

(4) Juris, A.; Balzani, V.; Barigelletti, F.; Belser, P.; von Zelewsky, A. *Coord. Chem. Res.* **1988**, *84*, 85.

(5) Kalyanasundaram, K.; Grätzel, M.; Pelizzetti, E. *Coord. Chem. Rev.* **1986**, *69*, 57.

(6) Krause, R. A. *Struct. Bonding* **1987**, *67*, 1.

(7) (a) Haga, M.; Matsumura-Inoue, T.; Yanabe, S. *Inorg. Chem.* **1987**, *26*, 4148. (b) Neyhart, G. A.; Meyer, T. J. *Inorg. Chem.* **1986**, *25*, 4807. (c) Hupp, J. T.; Neyhart, G. A.; Meyer, T. J. *J. Am. Chem. Soc.* **1986**, *108*, 5349. (d) Furue, M.; Kinoshita, S.; Kishida, T. *Chem. Lett.* **1987**, 2355. (e) Kalyanasundaram, K.; Nazeeruddin, Md. K. *Chem. Phys. Lett.* **1989**, *158*, 45.

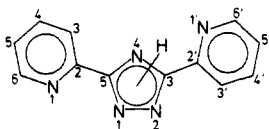
(8) Sahai, R.; Baucom, D. A.; Rillema, D. P. *Inorg. Chem.* **1986**, *25*, 3843. (9) (a) Kober, E. M.; Goldsby, K. A.; Narayana, D. N. S.; Meyer, T. J. *J. Am. Chem. Soc.* **1983**, *105*, 4303. (b) Schanze, K. S.; Neyhart, G. A.; Meyer, T. J. *J. Phys. Chem.* **1986**, *90*, 2182.

(10) Goldsby, K. A.; Meyer, T. J. *Inorg. Chem.* **1984**, *23*, 3002.

(11) (a) Kober, E. M. Thesis, North Carolina, 1982. (b) Kober, E. M.; Meyer, T. J. *Inorg. Chem.* **1984**, *23*, 3877. (c) Kober, E. M.; Meyer, T. J. *Inorg. Chem.* **1982**, *21*, 3967.

(12) (a) Curtis, J. C.; Bernstein, J. S.; Meyer, T. J. *Inorg. Chem.* **1985**, *24*, 385. (b) Schanze, K. S.; Meyer, T. J. *Inorg. Chem.* **1985**, *24*, 2122.

Recently, we reported the properties of $[\text{Ru}(\text{bpy})_2(\text{bpt})]^+$ and of the dinuclear species $[(\text{Ru}(\text{bpy})_2)_2(\text{bpt})]^{3+}$ with $\text{Hbpt} = 3,5$ -bis(pyridin-2-yl)-1,2,4-triazole.^{14a,b} For $[(\text{Ru}(\text{bpy})_2)_2(\text{bpt})]^{3+}$,



$\text{Hbpt} = 3,5$ -bis(pyridin-2-yl)-1,2,4-triazole

a large difference of 300 mV was observed between the two metal-based oxidation potentials. In this contribution we report the synthesis and physical properties of the two heteronuclear compounds of the type $[(\text{bpy})_2\text{M}(\text{bpt})\text{M}'(\text{bpy})_2]^{3+}$, where M and $\text{M}' = \text{Ru}$ or Os. In the first compound the ruthenium ion is bound via N(1) of the central triazole ring and osmium via N(4), while in the second isomer ruthenium is bound via N(4) and the osmium ion via N(1) of triazole. If the chemical environment induces a difference in oxidation potential, then the electrochemical properties of the two isomers should be different. Furthermore, the extent of delocalization will be studied for these systems and related to similar systems reported before. The X-ray structures of the ruthenium dinuclear systems and a mixed-metal ruthenium-osmium compound are reported, together with NMR data. It will be shown that the structures of the dinuclear systems are similar.

Experimental Section

Synthesis and Materials. 3,5-Bis(pyridin-2-yl)-1,2,4-triazole (Hbpt) was prepared according to literature methods.¹⁵ The compounds *cis*- $\text{Ru}(\text{bpy})_2\text{Cl}_2 \cdot 2\text{H}_2\text{O}$ and *cis*- $\text{Os}(\text{bpy})_2\text{Cl}_2$ were prepared according to literature methods.^{16,17} $[\text{Ru}(\text{bpy})_2(\text{bpt})]\text{PF}_6$, $[(\text{Ru}(\text{bpy})_2)_2(\text{bpt})](\text{PF}_6)_3$, $[\text{Os}(\text{bpy})_2(\text{bpt})]\text{PF}_6$, and $[(\text{Os}(\text{bpy})_2)_2(\text{bpt})](\text{PF}_6)_3$ were synthesized as reported elsewhere.¹⁴ The purity of all compounds was checked carefully by using NMR spectroscopy, electrochemical measurements, and elemental analysis.

$[(\text{bpy})_2\text{Ru}(\text{bpt})\text{Os}(\text{bpy})_2](\text{PF}_6)_3$, 0.5 mmol of $[\text{Ru}(\text{bpy})_2(\text{bpt})]\text{PF}_6$, and 0.5 mmol of $[\text{Os}(\text{bpy})_2\text{Cl}_2]$ were refluxed in alcohol-water (1/1 v/v) for 24 h. The hot solution was filtered and evaporated until dry. The residuum was subsequently dissolved in 10 mL of water. The dark solution was put on to a Sephadex SP-25 column and eluted with 3 M NaCl solution. The compound was precipitated by adding an excess of $\text{NH}_4\text{PF}_6 \cdot \text{H}_2\text{O}$ to the solution. After filtration, the compound was further purified by column chromatography with neutral alumina and ethanol as eluent. Finally, the complex was recrystallized from acetone-water.

$[(\text{bpy})_2\text{Os}(\text{bpt})\text{Ru}(\text{bpy})_2](\text{PF}_6)_3$, 0.5 mmol of $[\text{Os}(\text{bpy})_2(\text{bpt})]\text{PF}_6$, and 0.5 mmol of $[\text{Ru}(\text{bpy})_2\text{Cl}_2]$ were refluxed in alcohol-water for 24 h. Purification took place as described for the synthesis of $[\text{Ru}(\text{bpy})_2(\text{bpt})\text{Os}(\text{bpy})_2](\text{PF}_6)_3$.

Single crystals of $[(\text{Ru}(\text{bpy})_2)_2(\text{bpt})](\text{CF}_3\text{SO}_3)_3 \cdot 4\text{H}_2\text{O}$ were obtained by adding an excess of $\text{NH}_4\text{CF}_3\text{SO}_3$ in 10 mL of water to 1 mmol of $[(\text{Ru}(\text{bpy})_2)_2(\text{bpt})]^{3+}$ in 30 mL of water.^{14a} After 5 min, 40 mL of acetone was added and the solution was slowly evaporated at room temperature.

Single crystals of $[(\text{bpy})_2\text{Ru}(\text{bpt})\text{Os}(\text{bpy})_2](\text{CF}_3\text{SO}_3)_3 \cdot 4\text{H}_2\text{O}$ were obtained by adding an excess of $\text{NH}_4\text{CF}_3\text{SO}_3$ in 10 mL of water to 0.5 mmol of $[(\text{bpy})_2\text{Ru}(\text{bpt})\text{Os}(\text{bpy})_2]^{3+}$ in 30 mL of water. After 5 min, 40 mL of acetone was added and the solution was slowly evaporated at room temperature, until dark rod-shaped crystals were formed. The dinuclear compounds will be abbreviated as RuRu for the $[(\text{Ru}$

Table I. Experimental Crystallographic Data of $[(\text{Ru}(\text{bpy})_2)_2(\text{bpt})](\text{CF}_3\text{SO}_3)_3 \cdot 4\text{H}_2\text{O}$ and $[\text{Ru}(\text{bpy})_2(\text{bpt})\text{Os}(\text{bpy})_2](\text{CF}_3\text{SO}_3)_3 \cdot 4\text{H}_2\text{O}$

| formula | $\text{Ru}_2\text{C}_{55}\text{N}_{13}\text{H}_{48}\text{F}_9\text{O}_{13}\text{S}_3$ | $\text{RuOsC}_{55}\text{N}_{13}\text{H}_{48}\text{F}_9\text{O}_{13}\text{S}_3$ |
|---|---|--|
| M_r | 1568.37 | 1657.50 |
| cryst dimen, mm | $0.30 \times 0.20 \times 0.13$ | $0.40 \times 0.10 \times 0.08$ |
| cryst symm | monoclinic | monoclinic |
| space group | $P2_1/c$ | $P2_1/c$ |
| a , Å | 13.510 (1) | 13.5802 (7) |
| b , Å | 16.110 (2) | 16.247 (2) |
| c , Å | 29.861 (4) | 30.043 (3) |
| β , deg | 99.225 (9) | 100.348 (6) |
| V , Å ³ | 6415 (1) | 6521 (1) |
| Z | 4 | 4 |
| $D(\text{calcd})$, g cm ⁻³ | 1.62 | 1.69 |
| 2θ range, deg | 2.50–50 | 2.50–50 |
| temp, K | 200 | 200 |
| reflens collect | $-13 \leq h \leq 13$, $0 \leq k \leq 16$, $0 \leq l \leq 29$ | $0 \leq h \leq 4$, $0 \leq k \leq 16$, $-29 \leq l \leq 29$ |
| tot no. of data | 6882 | 2731 |
| no. of obsd data, $I > [2.5\sigma(I)]$ | 4218 | 1758 |
| $\mu(\text{Cu K}\alpha)$, cm ⁻¹ | 56.5 | 72.6 |
| R | 0.071 | 0.079 |
| R_w | 0.084 ^a | 0.131 ^b |
| $F(000)$ | 3160 | 3288 |

^a $R_w = [\sum w(|F_o| - |F_c|)^2 / \sum wF_o^2]^{1/2}$; $w = 1/\sigma_F^2$. ^b $R_w = [\sum w(|F_o| - |F_c|)^2 / \sum wF_o^2]^{1/2}$; $w = 9.08 + F_{\text{obs}} + 0.014F_{\text{obs}}^2$.

$(\text{bpy})_2(\text{bpt})]^{3+}$ cation, OsOs for the $[(\text{Os}(\text{bpy})_2)_2(\text{bpt})]^{3+}$ cation, RuOs for the $[(\text{bpy})_2\text{Ru}(\text{bpt})\text{Os}(\text{bpy})_2]^{3+}$ cation, and OsRu for the $[(\text{bpy})_2\text{Os}(\text{bpt})\text{Ru}(\text{bpy})_2]^{3+}$ cation.

Physical Measurements. UV-vis absorption spectra were recorded in ethanol on a Perkin-Elmer 330 spectrophotometer with 1-cm quartz cells. Proton NMR spectra were obtained on a Jeol JNM-FX 200-MHz spectrometer. All measurements were carried out in $(\text{CD}_3)_2\text{CO}$, with TMS as reference. COSY experiments were performed on a Bruker WM 300-MHz spectrophotometer. Further experimental details of the COSY measurements are given in a previous paper.^{14a} Electrochemical measurements were carried out in a microelectrode cell unit, using an E.G. and G. Par C Model 303 with an EG&G 384B polarographic analyzer. A saturated calomel electrode was used as reference electrode. The electrolyte used was acetonitrile containing 0.1 M tetrabutylammonium perchlorate (TBAP). A pulse height of 20 mV for the differential pulse measurements was used with a scan rate of 4 mV/s. For the cyclic voltammograms the scan rate was 100 mV/s.

Preparation of the Mixed-Valence Species. Electrochemical oxidation was carried out in a homemade three-compartment cell with a platinum sheet as working electrode, a calomel reference electrode, and a platinum wire as auxiliary electrode. The electrolyte used was acetonitrile containing 0.1 M tetrabutylammonium perchlorate. A Metrohm E524 Coulostat was used to carry out the bulk electrolysis experiments. Near-infrared spectra were obtained by using a Perkin-Elmer 330 spectrophotometer. The potentials applied for the preparation of the mixed-valence species were 1.20 V for RuRu, 0.75 V for OsOs, and 1.00 V vs SCE for the RuOs and OsRu complexes. The $\text{M}^{\text{III}}\text{M}^{\text{III}}$ species were obtained by oxidizing at 1.20 V for OsOs and 1.60 V for the RuRu, RuOs, and OsRu complexes.

X-ray Structure Determination of $[(\text{Ru}(\text{bpy})_2)_2(\text{bpt})](\text{CF}_3\text{SO}_3)_3 \cdot 4\text{H}_2\text{O}$ and $[\text{Ru}(\text{bpy})_2(\text{bpt})\text{Os}(\text{bpy})_2](\text{CF}_3\text{SO}_3)_3 \cdot 4\text{H}_2\text{O}$. Data collection of both compounds was performed on an ENRAF-NONIUS CAD4 diffractometer equipped with Cu K α radiation ($\lambda = 1.5418$ Å) at -73 °C. The structure of $[(\text{Ru}(\text{bpy})_2)_2(\text{bpt})](\text{CF}_3\text{SO}_3)_3 \cdot 4\text{H}_2\text{O}$ was solved by standard heavy-atom techniques and refined by using full-matrix least-squares refinements based on F with weights $w = 1/(2\sigma(F_o))$.^{18a} Absorption correction was applied by using the program DIFABS.^{18b} The positions of the hydrogen atoms were calculated on the basis of standard geometry and refined isotropically. All non-hydrogen atoms were refined anisotropically. The triflate groups showed disorder, and two positions for each triflate group were located by using electron density maps. Atomic scattering factors for neutral atoms were taken from the literature.^{18c}

(18) (a) Steward, J. M.; Machin, P. A.; Dickinson, C. W.; Ammon, H. L.; Heck, H.; Flack, H. *The X-RAY76 system*; Tech. Rep. TR-446; Computer Science Centre, University of Maryland, College Park, Maryland. (b) Walker, W.; Stuart, D. *Acta Crystallogr.* **1983**, *A39*, 158. (c) *International Tables for X-ray Crystallography*; Kynoch Press: Birmingham, England, 1974; Vol. IV.

(13) (a) Hush, N. S. *Prog. Inorg. Chem.* **1967**, *8*, 391. (b) Hush, N. S. *Electrochim. Acta* **1968**, *13*, 1005.

(14) (a) Hage, R.; Dijkhuis, A. H. J.; Haasnoot, J. G.; Prins, R.; Reedijk, J.; Buchanan, B. E.; Vos, J. G. *Inorg. Chem.* **1988**, *27*, 2185. (b) Hage, R.; Haasnoot, J. G.; Stufkens, D. J.; Snoeck, T. L.; Vos, J. G.; Reedijk, J. *Inorg. Chem.* **1989**, *28*, 1413. (c) Hage, R.; de Graaff, R. A. G.; Haasnoot, J. G.; Turkenburg, J. P.; Reedijk, J.; Vos, J. G. *Acta Crystallogr. C* **1989**, *45*, 381. (d) Barigelletti, F.; De Cola, L.; Balzani, V.; Hage, R.; Haasnoot, J. G.; Reedijk, J.; Vos, J. G. *Inorg. Chem.* **1989**, *28*, 4344. (e) Barigelletti, F.; De Cola, L.; Balzani, V.; Hage, R.; Haasnoot, J. G.; Reedijk, J.; Vos, J. G. *Inorg. Chem.* Submitted for publication.

(15) Geldard, J. F.; Lions, F. *J. Org. Chem.* **1965**, *30*, 318.

(16) Sullivan, B. P.; Salmon, D. J.; Meyer, T. *J. Inorg. Chem.* **1978**, *17*, 3334.

(17) Lay, P. A.; Sargeson, A. M.; Taube, H.; Chou, M. H.; Creutz, C. *Inorg. Synth.* **1986**, *24*, 291.

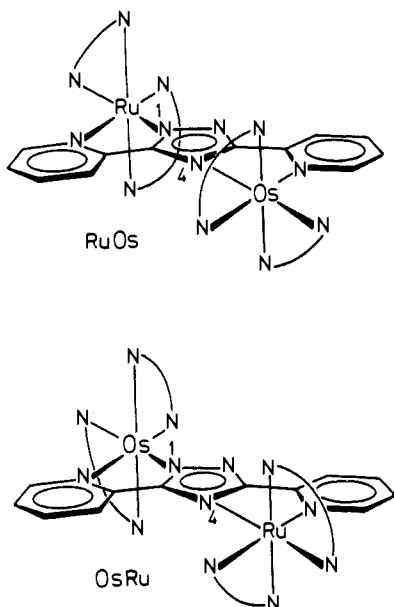
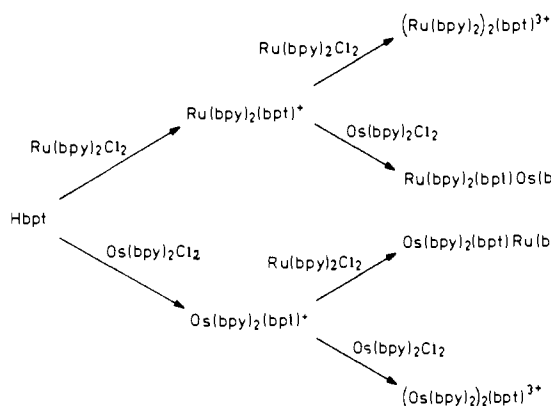


Figure 1. Structures of $[(\text{bpy})_2\text{Ru}(\text{bpt})\text{Os}(\text{bpy})_2]^{3+}$ (RuOs) and $[(\text{bpy})_2\text{Os}(\text{bpt})\text{Ru}(\text{bpy})_2]^{3+}$ (OsRu). In each case, only one geometrical isomer is drawn in the figure.

Scheme I. Reaction Scheme of the Synthesis of the Two Isomeric RuOs Compounds



The unit-cell data of $[(\text{Ru}(\text{bpy})_2(\text{bpt})\text{Os}(\text{bpy})_2)(\text{CF}_3\text{SO}_3)_3 \cdot 4\text{H}_2\text{O}]$ are similar to $[(\text{Ru}(\text{bpy})_2)_2(\text{bpt})](\text{CF}_3\text{SO}_3)_3 \cdot 4\text{H}_2\text{O}$, indicating an isomorphous replacement. Therefore, the atomic coordinates of $[(\text{Ru}(\text{bpy})_2)_2(\text{bpt})](\text{CF}_3\text{SO}_3)_3 \cdot 4\text{H}_2\text{O}$ were used to solve the structure of $[(\text{Ru}(\text{bpy})_2(\text{bpt})\text{Os}(\text{bpy})_2)(\text{CF}_3\text{SO}_3)_3 \cdot 4\text{H}_2\text{O}]$. Three cycles of isotropic refinement after the substitution of Ru(1) by Os(1) led to an *R* value of 19.3% with a negative temperature factor for Ru(2). The same procedure for the replacement of Ru(2) by Os(2) resulted in an *R* factor of 9.2% with normal temperature factors for both metal atoms. Due to the small amount of data for $[(\text{Ru}(\text{bpy})_2(\text{bpt})\text{Os}(\text{bpy})_2)(\text{CF}_3\text{SO}_3)_3 \cdot 4\text{H}_2\text{O}]$ no attempt was made to determine the hydrogen atoms, and the temperature factors were kept isotropic for all atoms. Details of crystal data, refinement, and intensity collection are given in Table I.

Results and Discussion

Synthesis of the Complexes. The outline of the syntheses of the two Ru-Os isomers with the bridging bispyridyltriazole ligand is presented in Scheme I. For the synthesis of the RuOs isomer, $[\text{Ru}(\text{bpy})_2(\text{bpt})]^+$ was treated with $[\text{Os}(\text{bpy})_2\text{Cl}_2]$ to yield the dinuclear compound. For the information of the second isomer (OsRu), $[\text{Os}(\text{bpy})_2(\text{bpt})]^+$ was treated with $[\text{Ru}(\text{bpy})_2\text{Cl}_2]$. To obtain pure compounds, it is important to use extremely pure mononuclear complexes. Therefore, before reacting the mononuclear complexes with a second $[\text{M}(\text{bpy})_2\text{Cl}_2]$ unit, the starting materials were carefully purified on a Sephadex SP-25 column by eluting with 0.1 M NaCl.¹⁴ Electrochemical and NMR measurements indicated a purity better than 98%. Earlier investigations have shown that the metal centers in $[\text{Ru}(\text{bpy})_2(\text{bpt})]^+$ and $[\text{Os}(\text{bpy})_2(\text{bpt})]^+$ only bind via N(1) of the triazole ring.^{14c}

Table II. Relevant Bond Distances and Angles of $[(\text{Ru}(\text{bpy})_2)_2(\text{bpt})](\text{CF}_3\text{SO}_3)_3 \cdot 4\text{H}_2\text{O}$ and Relevant Bond Distances for $[\text{Ru}(\text{bpy})_2(\text{bpt})\text{Os}(\text{bpy})_2](\text{CF}_3\text{SO}_3)_3$

| $[(\text{Ru}(\text{bpy})_2)_2(\text{bpt})](\text{CF}_3\text{SO}_3)_3 \cdot 4\text{H}_2\text{O}$ | | | | | |
|---|-----------|-------------------|-----------|-------------|----------|
| Bond Distances (Å) | | | | | |
| Ru(1)-N(1) | 2.03 (1) | Ru(1)-N(40) | 2.04 (1) | Ru(2)-N(60) | 2.06 (1) |
| Ru(1)-N(6) | 2.06 (1) | Ru(1)-N(46) | 2.06 (1) | Ru(2)-N(66) | 2.07 (1) |
| Ru(1)-N(20) | 2.07 (2) | Ru(2)-N(4) | 2.11 (1) | Ru(2)-N(80) | 2.07 (1) |
| Ru(1)-N(26) | 2.04 (1) | Ru(2)-N(12) | 2.10 (1) | Ru(2)-N(86) | 2.02 (1) |
| Angles (deg) | | | | | |
| N(1)-Ru(1)-N(6) | 77.6 (5) | N(4)-Ru(2)-N(12) | 77.2 (5) | | |
| N(1)-Ru(1)-N(20) | 92.8 (5) | N(4)-Ru(2)-N(60) | 85.1 (5) | | |
| N(1)-Ru(1)-N(26) | 97.9 (5) | N(4)-Ru(2)-N(66) | 103.0 (5) | | |
| N(1)-Ru(1)-N(40) | 93.6 (5) | N(4)-Ru(2)-N(80) | 97.7 (5) | | |
| N(1)-Ru(1)-N(46) | 169.8 (6) | N(4)-Ru(2)-N(86) | 172.8 (6) | | |
| N(6)-Ru(1)-N(20) | 96.4 (6) | N(12)-Ru(2)-N(60) | 94.1 (5) | | |
| N(6)-Ru(1)-N(40) | 173.2 (5) | N(12)-Ru(2)-N(66) | 174.1 (6) | | |
| N(6)-Ru(1)-N(46) | 88.2 (6) | N(12)-Ru(2)-N(80) | 89.1 (5) | | |
| N(6)-Ru(1)-N(46) | 94.5 (5) | N(12)-Ru(2)-N(86) | 96.7 (6) | | |
| N(20)-Ru(1)-N(26) | 78.6 (6) | N(60)-Ru(2)-N(66) | 80.0 (6) | | |
| N(20)-Ru(1)-N(40) | 172.7 (5) | N(60)-Ru(2)-N(80) | 176.2 (5) | | |
| N(20)-Ru(1)-N(46) | 94.6 (6) | N(60)-Ru(2)-N(86) | 99.3 (6) | | |
| N(26)-Ru(1)-N(40) | 97.1 (6) | N(66)-Ru(2)-N(80) | 96.7 (6) | | |
| N(26)-Ru(1)-N(46) | 90.5 (5) | N(66)-Ru(2)-N(86) | 83.4 (6) | | |
| N(40)-Ru(1)-N(46) | 79.5 (6) | N(80)-Ru(2)-N(86) | 78.1 (6) | | |

| $[\text{Ru}(\text{bpy})_2(\text{bpt})\text{Os}(\text{bpy})_2](\text{CF}_3\text{SO}_3)_3$ | | | | | |
|--|----------|-------------|----------|-------------|----------|
| Bond Distances (Å) | | | | | |
| Ru(1)-N(1) | 2.07 (2) | Ru(1)-N(40) | 1.99 (5) | Os(2)-N(60) | 2.02 (5) |
| Ru(1)-N(6) | 2.08 (4) | Ru(1)-N(46) | 2.04 (3) | Os(2)-N(66) | 2.05 (3) |
| Ru(1)-N(20) | 2.06 (4) | Os(2)-N(4) | 2.10 (2) | Os(2)-N(80) | 2.09 (5) |
| Ru(1)-N(26) | 2.24 (4) | Os(2)-N(12) | 2.01 (3) | Os(2)-N(86) | 2.02 (3) |

Table III. Proton NMR Data of the Dinuclear Compounds^a

| | H3 | H4 | H5 | H6 | H3' | H4' | H5' | H6' |
|------|------|------|------|------|------|------|------|------|
| RuRu | 6.69 | 7.33 | 7.21 | 7.82 | 8.73 | 8.08 | 7.29 | 7.11 |
| OsRu | 6.57 | 7.12 | 7.08 | 7.75 | 8.69 | 7.87 | 7.20 | 7.08 |
| RuOs | 6.77 | 7.31 | 7.21 | 7.84 | 8.79 | 8.03 | 7.33 | 7.04 |

^a Measured in *d*⁶-acetone; values in ppm vs TMS. The chemical shifts of the protons of bpt of one geometrical isomer are listed.

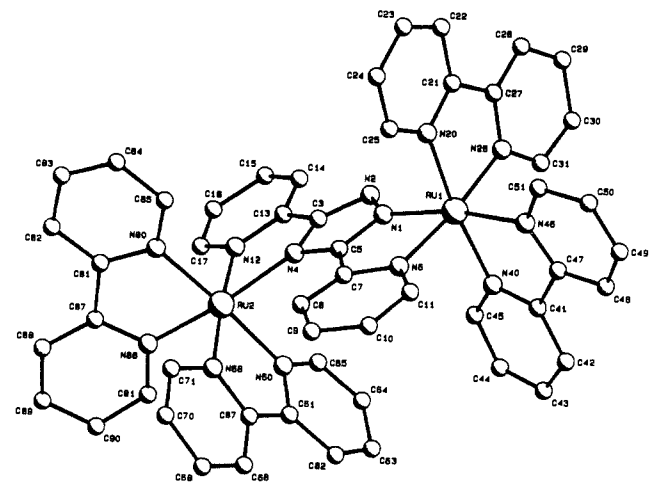


Figure 2. PLUTO drawing of the $[(\text{Ru}(\text{bpy})_2)_2(\text{bpt})]^{3+}$ cation. All hydrogens atoms have been omitted for reasons of clarity. Ellipsoids are drawn at 50% probability.

As a result the osmium unit in the RuOs compound is expected to be bound via N(4) to the triazole ring. For the OsRu compound, the osmium center is bound via N(1) and the ruthenium ion via N(4) (Figure 1).

Description of the Crystal Structures of $[(\text{Ru}(\text{bpy})_2)_2(\text{bpt})](\text{CF}_3\text{SO}_3)_3 \cdot 4\text{H}_2\text{O}$ and $[\text{Ru}(\text{bpy})_2(\text{bpt})\text{Os}(\text{bpy})_2](\text{CF}_3\text{SO}_3)_3 \cdot 4\text{H}_2\text{O}$. Fractional atomic coordinates are given in Table II. In Table III, relevant bond distances and angles are presented. Figure 2 shows a PLUTO¹⁹ diagram of the structure of $[(\text{Ru}(\text{bpy})_2)_2(\text{bpt})](\text{CF}_3\text{SO}_3)_3 \cdot 4\text{H}_2\text{O}$. The ruthenium-nitrogen distances of

(19) Motherwell, W. D. S.; Clegg, W. PLUTO. Program for plotting molecular and crystal structure; University of Cambridge, UK.

Table IV. Visible Absorption Spectra (Measured in Ethanol) of the Ruthenium–Osmium Compounds with Bispyridyltriazole

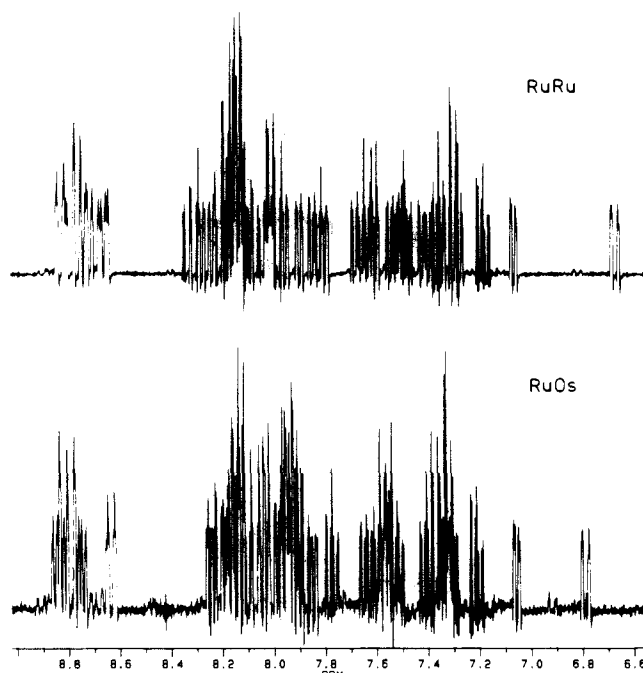
| compd | λ_{\max}^a (ϵ , $\times 10^4$) |
|---|--|
| [Ru(bpy) ₂ (bpt)] ⁺ | 475 (1.13) ^{14b} |
| [Os(bpy) ₂ (bpt)] ⁺ | 610 (0.28), 486 (1.08), 438 (1.06), 392 (1.34) ^{14c} |
| [(Ru(bpy) ₂) ₂ (bpt)] ³⁺ | 452 (2.26) ^{14b} |
| [(Os(bpy) ₂) ₂ (bpt)] ³⁺ | 660 (sh), 600 (0.44), 475 (1.82), 460 (1.82), 442 (1.72), 393 (1.76) ^{14c} |
| [(bpy) ₂ Ru(bpt)Os(bpy) ₂] ³⁺ | 660 (sh), 600 (sh), 459 (2.38), 394 (sh) |
| [(bpy) ₂ Os(bpt)Ru(bpy) ₂] ³⁺ | 670 (sh), 580 (sh), 453 (2.37) |

^ash = shoulder.

2.02–2.12 Å observed in this compound are in their normal range.^{14c,20} The electrochemical data suggest that the N(1) site of the triazole ring is a better σ -donor than the N(4) site (vide supra). This is confirmed by the structural data, as the Ru(1)–N(1) distance is significantly shorter than Ru(2)–N(4). The distances and angles of the bipyridyl ligands are in the normal range for Ru(bpy)₂ complexes and have been listed in tables in the supplementary material.^{14c,20} The “bite-angle” of the chelating ligands is between 77° and 80°, which is also typical for bipyridine-like ligands.^{14c,20} The angles between the triazole ring and the two pyridine rings of the bpt ligand are 9.8 (7°) between N(1)–C(5) and N(6)–C(12) and 14.3 (4°) between N(1)–C(5) and N(12)–C(17). The angles between the pyridine rings of the four bpy ligands are 5.7 (7°) (N(20)–C(31)), 3.2 (7°) (N(40)–C(51)), 9.7 (6°) (N(60)–C(71)), and 8.5 (7°) (N(80)–C(91)). The data indicate that the bpy ligands are less distorted from planarity than the bpt ligand; a considerable distortion of the bpt ligand is present after coordination with two Ru(bpy)₂ moieties. This distortion is much larger than observed for the mononuclear [Ru(bpy)₂(bpt)]PF₆,^{14c} where the angles between the rings of the bpt ligand are about 3°.

Despite the small amount of X-ray data obtained for [Ru(bpy)₂(bpt)Os(bpy)₂](CF₃SO₃)₃·4H₂O, it is clear that the osmium–nitrogen distances are roughly the same as the ruthenium–nitrogen distances. This has been observed before for [M(bpy)₃]²⁺ with Ru–N and Os–N distances of 2.056 Å.^{20f,g} For [(Ru(bpy)₂)₂(bpt)](CF₃SO₃)₃·4H₂O the metal–metal distance is 6.184 (2) Å, and for [Ru(bpy)₂(bpt)Os(bpy)₂](CF₃SO₃)₃·4H₂O the Ru(1)–Os(2) distance is 6.161 (4) Å. The similarity in metal–metal distances shows the close resemblance of the structures of the two compounds. These distances will be used below for the calculation of the extent of electron delocalization present for the dinuclear systems.

¹H NMR analysis of the X-ray samples has shown that in these fractions only one isomer is present (vide infra), having a structure as is given in Figure 1. From previous NMR studies^{14a} of the ruthenium dinuclear compound, it was already concluded that two geometrical isomers are formed upon heating Hbpt with an excess of [Ru(bpy)₂Cl₂]. Careful crystallization of the product obtained allowed that two geometrical isomers could be separated. The second geometrical isomer has not been isolated in pure crystalline state with the triflate anions, but it is probably formed in the same amount as the first geometrical isomer. For each geometrical isomer an optical isomer is present.^{14a} So, for each dinuclear compound (RuRu, RuOs, OsRu, and OsOs) four isomers are formed. The X-ray structures confirm the presence of the optical isomers, because in P₂/c each molecule has its optical isomer in the unit cell. No attempts have been carried out to separate the optical isomers of the compounds. All measurements as discussed in the next section were carried out on the mixtures of

**Figure 3.** ¹H NMR spectra of one isomer of [(bpy)₂Ru(bpt)Os(bpy)₂]³⁺ and [(Ru(bpy)₂)₂(bpt)]³⁺.^{14a}

the aforementioned geometrical and optical isomers.

¹H NMR Spectroscopy. Previously an elaborate discussion has been given on the NMR spectra of the ruthenium mononuclear and dinuclear compounds.^{14a} Because of the structural similarities between the dinuclear compounds, the NMR spectra of the heteronuclear compounds should be similar to the spectrum of RuRu. As shown in Table IV and Figure 3, the NMR spectra are indeed very alike. The doublet at 6.57–6.77 ppm is noteworthy, as it has previously been shown^{14a} that this proton has a very short distance to an adjacent bpy ligand, thus yielding a strong upfield shift. In contrast to what was reported before,^{14a} the signals at around 7.1 ppm are due to H6' protons of the second pyridine rings of bpt and not due to the H3' protons. As shown in Figure 3, the coupling constant of the signal of H6' around 7.1 ppm is smaller than that of the H3' doublet at 6.6 ppm. The same observation has been made for [Ru(bpy)₂(pyridine)₂]²⁺, where the assignment has been made by using 2D techniques and isotopic labeling experiments.^{20c} By using 2D-COSY techniques, the assignments of the other protons of the bpt ligand for the two mixed-metal complexes was straightforward. The most important conclusion from these data is that the structures of the three compounds are very similar, as is also concluded from the X-ray data of [(Ru(bpy)₂)₂(bpt)](CF₃SO₃)₃·4H₂O and [Ru(bpy)₂(bpt)Os(bpy)₂](CF₃SO₃)₃·4H₂O. The only difference between the RuOs and OsRu compounds is that in the RuOs complex ruthenium is bound via N(1) and osmium via N(4) of the triazole ring, while in the OsRu compound, osmium is bound via N(1) and ruthenium via N(4) of the bpt ligand. This conclusion is of paramount importance for the discussion of the electrochemical data. A schematic presentation of the dinuclear compounds is given in Figure 1.

Absorption Spectra. Table V lists λ_{\max} and extinction coefficients of the RuOs and OsRu compounds with bispyridyltriazole. For comparison, the data of [Ru(bpy)₂(bpt)]PF₆^{14a} and [(Ru(bpy)₂)₂(bpt)](PF₆)₃^{14a} and [Os(bpy)₂(bpt)]PF₆^{14c} and [(Os(bpy)₂)₂(bpt)](PF₆)₃^{14c} are included. The intense absorption bands between 350 and 500 nm have been assigned as metal-to-ligand charge-transfer bands (MLCT).^{10–12} At lower energy, some additional bands are visible for the compounds containing osmium. These bands have been observed before for other osmium complexes, and have been assigned as forbidden transitions to triplet states.¹² The MLCT bands of the RuOs and OsRu compounds are very similar, both showing weak bands at the low-energy side and a strong MLCT band at around 460 nm (Table V). The

(20) (a) Boone, S. R.; Pierpont, C. G. *Inorg. Chem.* **1987**, *26*, 1769. (b) Eggleston, D. S.; Goldsby, K. A.; Hodgson, D. J.; Meyer, T. J. *Inorg. Chem.* **1985**, *24*, 4573. (c) Rillema, D. P.; Taghdiri, D. G.; Jones, D. S.; Keller, C. D.; Worl, L. A.; Meyer, T. J. *Inorg. Chem.* **1987**, *26*, 578. (d) Hitchcock, P. B.; Seddon, K. R.; Turp, J. E.; Yousif, Y. Z.; Zora, J. A.; Constable, E. C.; Wernberg, O. *J. Chem. Soc., Dalton Trans.* **1988**, 1837. (e) Heeg, M. J.; Kroener, R.; Deutsch, E. *Acta Crystallogr., Sect. C* **1985**, *41*, 684. (f) Constable, E. C.; Raithby, P. R.; Smit, D. N. *Polyhedron*, **1989**, *8*, 367. (g) Rillema, D. P.; Jones, D. S.; Levy, H. A. *J. Chem. Soc., Chem. Commun.* **1979**, 849.

Table V. Electrochemical Data of the Various Complexes Containing Bispyridyltriazole^a

| compd | oxidation potential | | $\Delta E_{1/2}$ reduction potential | | | | | | |
|---|---------------------|------|--------------------------------------|-------|-------|-------|----------------------|----------------------|-------|
| | | | | | | | | | |
| [Os(bpy) ₂ (bpt)] ⁺ | 0.49 | | -1.41 | -1.69 | -2.22 | -2.37 | -2.49 ^{14c} | | |
| [Ru(bpy) ₂ (bpt)] ⁺ | 0.85 | | -1.47 | -1.72 | -2.28 | -2.45 | -2.52 ^{14b} | | |
| [(Os(bpy) ₂) ₂ (bpt)] ³⁺ | 0.64 | 0.85 | 0.21 | -1.34 | -1.57 | -2.23 | -2.30 ^{14c} | | |
| [(Ru(bpy) ₂) ₂ (bpt)] ³⁺ | 1.04 | 1.34 | 0.30 | -1.40 | -1.62 | -1.67 | -2.23 | -2.33 ^{14b} | |
| [(bpy) ₂ Ru(bpt)Os(bpy) ₂] ³⁺ | 0.73 | 1.20 | 0.47 | -1.33 | -1.41 | -1.59 | -1.69 | -2.15 | -2.32 |
| [(bpy) ₂ Os(bpt)Ru(bpy) ₂] ³⁺ | 0.65 | 1.30 | 0.65 | -1.36 | -1.63 | -2.17 | -2.32 | | |

^aAll compounds have been measured in acetonitrile with 0.1 M NBu₄PF₆. The oxidation and reduction potentials (V vs SCE) have been determined with differential pulse polarography. $\Delta E_{1/2}$ is defined as the difference between the two oxidation potentials of the dinuclear systems.

Table VI. Properties of the Intervalence Transition of the Mixed-Valence Dinuclear Compounds Measured in CH₃CN^a

| | E_{op} | E_{op}^b | ϵ_{max} | $\Delta\nu_{1/2}^{exp}$ | $\Delta\nu_{1/2}^{calc}$ | α^2 |
|------------------------------------|----------|------------|------------------|-------------------------|--------------------------|-------------------------------|
| Ru ^{III} Ru ^{II} | 5556 | 5730 | 2400 | 3300 | 3341 | 1.6×10^{-2} |
| Ru ^{II} Os ^{III} | 7143 | 7100 | 1200 | 3800 | 3650 | 7.0×10^{-3} |
| Os ^{III} Ru ^{II} | 8772 | 8556 | 1140 | 4300 | 3700 | 6.1×10^{-3} |
| Os ^{III} Os ^{II} | 8333 | | 460 | 4500 | 4170 | 2.7×10^{-3} |
| | 5000 | | 440 ^c | 3500 | 3144 | 3.4×10^{-3} |
| | | | | | | $\Sigma = 6.1 \times 10^{-3}$ |

^a E_{op} and $\Delta\nu_{1/2}$ in cm⁻¹, ϵ_{max} in M⁻¹ cm⁻¹. ^bValues between parentheses are the energies of the IT band calculated by using eq 3. ^cCorrected for dπ-dπ transitions of the osmium(III) center.

absorption at 459 and 453 nm is caused by both Ru → π*(bpy) and Os → π*(bpy) transitions.

Electrochemical Measurements. In Table VI, the electrochemical data of the mixed-metal compounds together with that of the homonuclear ruthenium and osmium compounds are presented.^{14a,d} As expected, the oxidation potentials of the osmium moieties are about 0.4 V lower than those in the ruthenium analogues.^{7,9,21-24} The difference in oxidation potentials of the mixed-metal compounds (RuOs) and (OsRu) gives information about the influence of the different coordination sites of the bridging triazole ligand. If both coordination sites are equivalent (N(1) + N(pyr) or N(4) + N(pyr)), then the oxidation potentials of the RuOs and OsRu dinuclear complexes should be similar. If not, differences in oxidation potentials are likely to be observed between the two compounds. The oxidation potentials of compounds (RuOs) and (OsRu) do indeed show quite large differences, indicating that differences in chemical environments must be important in this system (Figure 4). The oxidation potentials of the ruthenium and osmium complexes containing bpt have been schematically depicted in Figure 5. In the RuOs dinuclear compound, the osmium ion bound to N(4) of the triazole ring is oxidized first at 0.73 V, while the N(1)-bound ruthenium ion is subsequently oxidized at 1.20 V. In the OsRu compound, osmium (now coordinated via N(1) of the triazole ring) is oxidized at the lower potential of 0.65 V, while the ruthenium ion is oxidized at a higher potential (1.30 V) than in the RuOs compound. This can be rationalized by assuming that the N(1) of the triazole ring is a better σ-donor than the N(4) atom. A ligand with strong σ-donor properties induces a lowering of the metal oxidation potential.⁴ The fact that the N(1) site of the triazole ring is a better σ-donor site than the N(4) site has recently been confirmed by measurements on two isomeric Ru(bpy)₂(pyridyltriazole) complexes.²⁵ The oxidation potential of the N(1) Ru(bpy)₂ center to the 3-(pyridin-2-yl)-1,2,4-triazole (ptr) ligand is 60–70 mV lower than that for the N(4) isomer.²⁵ It is interesting to note that the first oxidation potential of the OsRu compound is nearly the same as the first potential of the OsOs compound (Table IV). The second oxidation potential of the OsRu compound is also similar to the second oxidation potential of the RuRu compound. This observation shows again that the N(1)-bounded metal center

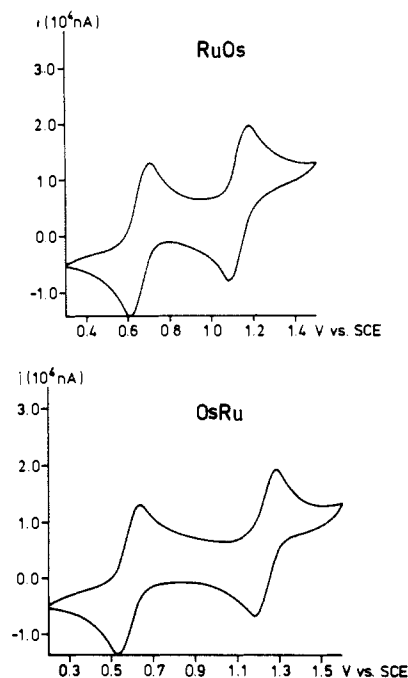


Figure 4. Cyclic voltammograms of the two mixed-metal dinuclear compounds containing bispyridyltriazole (bpt), measured in acetonitrile. All values are vs SCE.

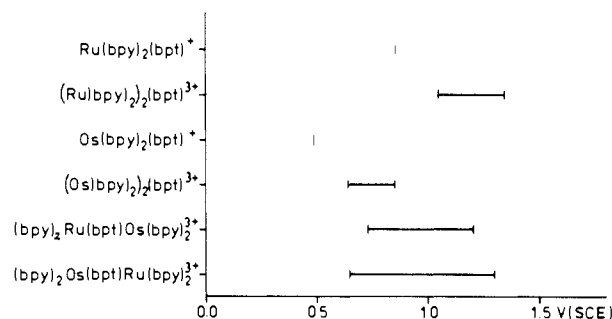


Figure 5. Schematic representation of the oxidation potentials of the various complexes containing deprotonated bpt: Ru = [Ru(bpy)₂(bpt)]⁺, Os = [Os(bpy)₂(bpt)]⁺, RuRu = [(Ru(bpy)₂)₂(bpt)]³⁺, RuOs = [(bpy)₂Ru(bpt)Os(bpy)₂]³⁺, OsRu = [(bpy)₂Os(bpt)Ru(bpy)₂]³⁺, and OsOs = [(Os(bpy)₂)₂(bpt)]³⁺.

is oxidized more easily than the N(4)-bounded metal ion.

The reduction potentials for the dinuclear compounds have similar values, although the splitting of the potentials at about -1.4 and -1.6 V of the RuOs dinuclear complexes is larger than those of [(Ru(bpy)₂)₂(bpt)]³⁺ (see Figure 6 and Table III). This is caused by the greater asymmetry in the RuOs mixed-metal compound compared to RuRu. The splitting of the two reduction peaks for the OsRu compound is not observed (see Table III). From resonance Raman measurements on [Ru(bpy)₂(bpt)]⁺ and [(Ru(bpy)₂)₂(bpt)]³⁺, it has been concluded that the lowest π* levels of those complexes are from bipyridine ligands and not from bpt ligands.^{14b} From the similarities in reduction behavior of all complexes, it has been concluded that the LUMO π* orbitals of

(21) Creutz, C.; Chou, M. H. *Inorg. Chem.* **1987**, *26*, 2995.

(22) Pipes, D. W.; Meyer, T. J. *Inorg. Chem.* **1984**, *23*, 2466.

(23) Kober, E. M.; Sullivan, B. P.; Dressick, W. J.; Casper, J. V.; Meyer, T. J. *J. Am. Chem. Soc.* **1980**, *102*, 7385.

(24) Bond, A. M.; Haga, M. *Inorg. Chem.* **1986**, *25*, 4507.

(25) Buchanan, B. E.; Wang, R.; Vos, J. G.; Hage, R.; Haasnoot, J. G.; Reedijk, J. *Inorg. Chem.* In press.

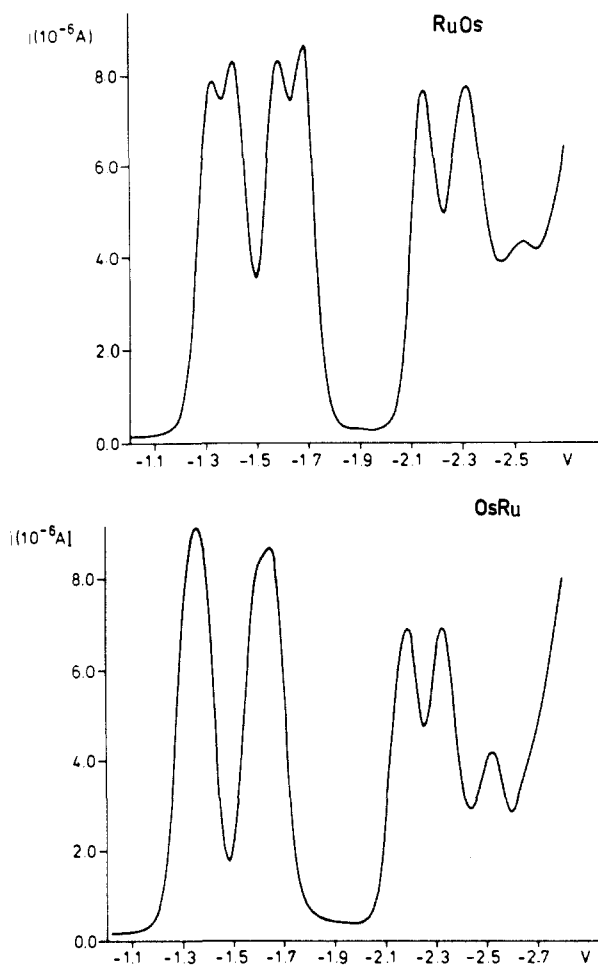


Figure 6. Differential pulse polarograms of reduction potentials of $[(\text{bpy})_2\text{Ru}(\text{bpt})\text{Os}(\text{bpy})_2]^{3+}$ and $[(\text{bpy})_2\text{Os}(\text{bpt})\text{Ru}(\text{bpy})_2]^{3+}$.

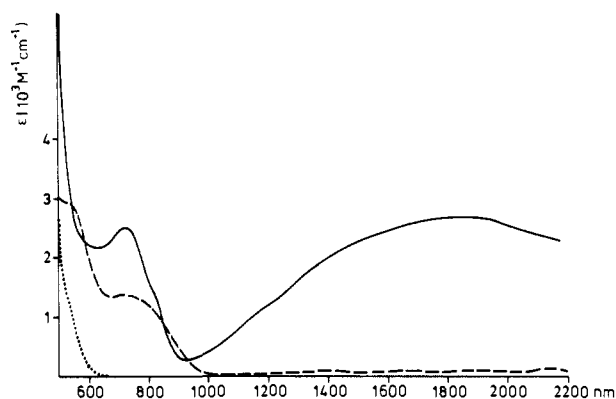


Figure 7. Near-infrared spectra of $[(\text{Ru}(\text{bpy})_2)_2(\text{bpt})]^{n+}$ on the electrochemical oxidation in CH_3CN (0.1 M TBAP) before electrolyses ($n = 3$ (···) at 1.20 V ($n = 4$ (—)) and at 1.60 V vs SCE ($n = 5$ (---)).

all complexes reported here are bpy based.

Mixed-Valence Compounds. Electrochemical oxidation of the dinuclear ruthenium compound to the mixed-valence species yields two new bands, at 735 and 1800 nm. Further oxidation to the $\text{Ru}^{\text{III}}\text{Ru}^{\text{III}}$ species causes a disappearance of the band at 1800 nm and a small shift of the band at 735 nm to 725 nm (see Figure 7). Initially it appeared that the band at 735 nm is caused by an intervalence transition (IT).^{14a} However, a band is still visible after full oxidation and, therefore, cannot be caused by an intervalence transition from the Ru^{II} to the Ru^{III} center. Comparison with literature data of analogous complexes with benzimidazolone ions suggests that the band around 735 nm in fact is a ligand-to-metal charge-transfer (LMCT) band.^{7a} The disappearance of the band at 1800 nm when the complex is fully oxidized shows

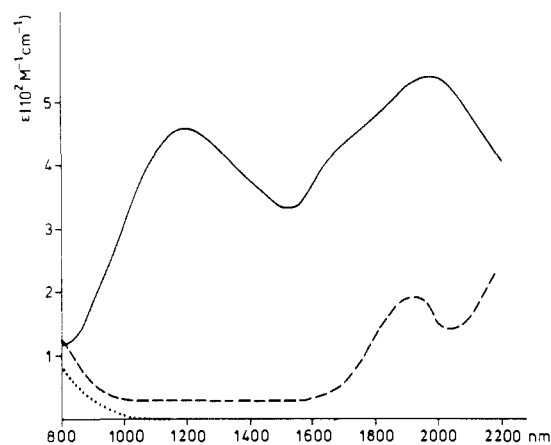


Figure 8. Near-infrared spectra of $[(\text{Os}(\text{bpy})_2)_2(\text{bpt})]^{n+}$ on the electrochemical oxidation in CH_3CN (0.1 M TBAP) before electrolyses ($n = 3$ (···) at 0.75 V ($n = 4$ (—)) and at 1.10 V vs SCE ($n = 5$ (---)).

that this band must be an IT band. Hush derived the properties of intervalence transitions in mixed-valence species, and he showed that the band at half-height of the IT band can be calculated by using eq 1,¹³ with $\Delta\nu_{1/2}$ the calculated band width at half height

$$\Delta\nu_{1/2} = [2310(E_{\text{op}} - \delta E)]^{1/2} \quad (1)$$

of the intervalence band, E_{op} the energy of the intervalence band, and δE the energy difference induced by the asymmetric coordination environment. This value has been estimated as 800 cm^{-1} from the electrochemical measurements on the two isomers $\text{Ru}(\text{bpy})_2(\text{pyridyltriazole})$ complexes (vide supra).²⁵

The measured and calculated band width agree very well, thus further substantiating the assumption that the band at 1800 nm is indeed an IT band (Table VI). By using eq 2,¹³ the extent of electron delocalization α^2 can be calculated, with α^2 the extent

$$\alpha^2 = \frac{(4.2 \times 10^{-4})\epsilon_{\text{max}}\Delta\nu_{1/2}}{d^2 E_{\text{op}}} \quad (2)$$

of electron delocalization, ϵ_{max} the extinction coefficient of the IT band ($\text{M}^{-1} \text{ cm}^{-1}$), and d the distance between the metal centers (6.184 Å). From this equation, a value of $\alpha^2 = 0.016$ has been obtained for the RuRu compound, suggesting that electron delocalization is significant.^{13,26} In fact, this value is very similar to the one found by Hage et al. for the mixed-valence $\text{Ru}(\text{bpy})_2$ species with a bisbenzimidazolone bridge.^{7a} Hage suggested that the stabilization of the mixed-valence species is caused by the strong σ -donor properties and the enhanced $d\pi(\text{M}^{\text{II}})-\pi(\text{L})$ mixing. The greater coupling for the RuRu compound suggests that the dominant electronic interaction between the metal centers is due to a $d\pi(\text{Ru}^{\text{II}})-\pi$ mixing rather than via $d\pi(\text{Ru}^{\text{II}})-\pi^*$ mixing.²⁷ It is likely that the suggestions made by Hupp²⁸ that hole transfer is of major importance on the extent of electron delocalization for such systems is justified.

The situation for the osmium dinuclear compound is more complicated as strong spin-orbit coupling can result in *three* IT bands. or several dinuclear osmium complexes two IT bands are observed between 2000 and 800 nm, while it is expected that the third one was obscured by the intense MLCT and LMCT bands at higher energy.^{7a} Figure 8 shows the near-infrared absorption spectra of the OsOs dinuclear complex after partial and full oxidation. For this compound two IT bands with a difference of 3200 cm^{-1} are present. As shown in Table VI, the calculated and measured band widths at half height agree very well for the two IT bands. The extent of electron delocalization has been calculated by using the parameters of both IT bands. As the high-energy

(26) Creutz *Prog. Inorg. Chem.* **1983**, 30, 1.

(27) We acknowledge one of the referees for this explanation of the observed behavior.

(28) Hupp, J. T. *J. Am. Chem. Soc.* **1990**, 112, 1563.

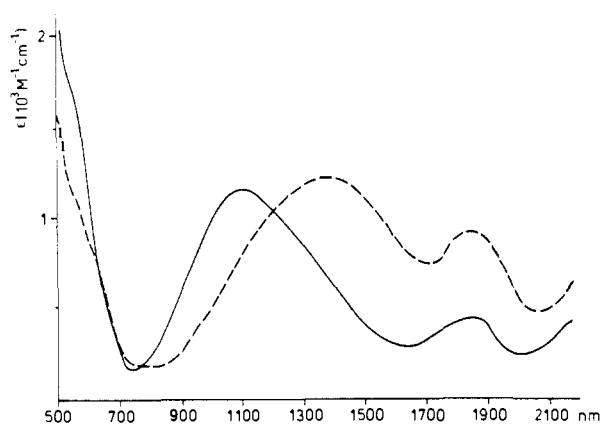


Figure 9. Near-infrared spectra of $[(\text{bpy})_2\text{Ru}(\text{bpt})\text{Os}(\text{bpy})_2]^{4+}$ (—) and $[(\text{bpy})_2\text{Os}(\text{bpt})\text{Ru}(\text{bpy})_2]^{4+}$ (---) in CN_3CN both oxidized at 1.00 V vs SCE.

band could not be measured the total extent of electron delocalization as given in Table VI is the lower limit. After full oxidation a weak $d\pi-d\pi$ band was visible at 5260 cm^{-1} ($\epsilon = 200\text{ M}^{-1}\text{ cm}^{-1}$). Due to the large spin-orbit coupling of the osmium ion, the d^5 orbitals are split and $d\pi-d\pi$ transitions are often present.⁷ For the determination of the extinction coefficient of the low-energy IT band for the mixed-valence species half of the intensity of the $d\pi-d\pi$ transition as observed for the $\text{Os}^{\text{III}}-\text{Os}^{\text{III}}$ species has been subtracted.

Also the properties of the mixed-valence heteronuclear bpt complexes (RuOs and OsRu) have been studied. The near-infrared absorption spectra of the mixed-valence $[(\text{bpy})_2\text{Ru}(\text{bpt})\text{Os}(\text{bpy})_2]^{4+}$ and $[(\text{bpy})_2\text{Os}(\text{bpt})\text{Ru}(\text{bpy})_2]^{4+}$ are presented in Figure 9. Goldsby and Meyer have shown that the energy of the IT band of a ruthenium-osmium complex with bipyrimidine (bpm) as bridging ligand can be calculated by using the energy of the IT band of the dinuclear ruthenium compound and the difference in oxidation potentials of the RuRu-bpm and RuOs-bpm compound.¹⁰ Therefore, the differences in structure and vibrational reorganization energies between the ruthenium and analogous osmium compounds must be very small.

As shown in the electrochemical section, the differences in oxidation potentials of the two metal centers ($\Delta E_{1/2}$) for the OsOs compound is 210 mV ($1.70 \times 10^3\text{ cm}^{-1}$), for the RuRu compound 300 mV ($2.42 \times 10^3\text{ cm}^{-1}$), for the RuOs compound 470 mV ($3.80 \times 10^3\text{ cm}^{-1}$), and for the OsRu complex 650 mV ($5.26 \times 10^3\text{ cm}^{-1}$). Defining $\Delta\Delta E_{1/2} = [\Delta E_{1/2}(\text{RuRu}) - \Delta E_{1/2}(\text{OsOs})]$ yields a value of 90 mV ($0.72 \times 10^3\text{ cm}^{-1}$) for the RuRu system with respect to the OsOs dimer. A similar calculation for the RuOs system with $\Delta\Delta E_{1/2} = [\Delta E_{1/2}(\text{RuOs}) - \Delta E_{1/2}(\text{OsOs})]$ yields a value of 260 mV ($2.10 \times 10^3\text{ cm}^{-1}$). For the OsRu system a value of 440 mV ($3.56 \times 10^3\text{ cm}^{-1}$) has been obtained. By using eq 3, the optical energy of the RuRu compound with respect to that of the OsOs compound can be calculated. Using $E_{\text{op}}(\text{OsOs}) = 5.0 \times$

$$E_{\text{op}}(\text{RuRu}) = E_{\text{op}}(\text{OsOs}) - [\Delta E_{1/2}(\text{OsOs}) - \Delta E_{1/2}(\text{RuRu})] \quad (3)$$

10^3 cm^{-1} (Table VI), $\Delta E_{1/2}(\text{OsOs}) = 1.70 \times 10^3\text{ cm}^{-1}$, $\Delta E_{1/2}(\text{RuRu}) = 2.42 \times 10^3\text{ cm}^{-1}$, $\Delta E_{1/2}(\text{RuOs}) = 3.80 \times 10^3\text{ cm}^{-1}$, and

$\Delta E_{1/2}(\text{OsRu}) = 5.26 \times 10^3\text{ cm}^{-1}$ yields the energies of the IT bands for the RuRu, RuOs, and OsRu compounds as presented in Table VI. The calculated values are in good agreement with the measured ones, thus showing that the analyses carried out for the bipyrimidine systems¹⁰ are also valid for the bispyridyltriazole complexes.

Interestingly, the extent of electron delocalization for the RuRu complex is much larger than that observed for the RuOs, OsRu, and OsOs complexes (Table VI). A similar observation has been made previously for complexes containing the bisbenzimidazole ligand^{7a} and has been explained by a greater overlap between the $d\pi(\text{Ru})-\pi(\text{L})$ orbitals than between the $d\pi(\text{Os})-\pi(\text{L})$ orbitals. This effect also causes a larger splitting in oxidation potentials for the RuRu dinuclear complex than for the OsOs compound, which has been observed both for the benzimidazole and for the bpt systems.

Conclusions

The X-ray structure determination and the NMR data of the RuRu, RuOs, and OsRu complexes and the NMR data show that the dinuclear systems are isostructural. The electrochemical data of the different homonuclear and heteronuclear compounds clearly show that the asymmetry of the triazole bridge has a large influence on the oxidation potentials. The N(1) site of the triazole ligand is a better σ -donor than the N(4) nitrogen atom, causing a destabilization of the filled d-orbitals (lower oxidation potential). The mixed-valence RuRu, RuOs, OsRu, and OsOs species exhibit rather intense intervalence transitions, and a clear correlation between the oxidation potentials and the energies of the IT bands for the RuRu, RuOs, and OsRu complexes has been observed. Although such correlation has been reported before for dinuclear systems with 2,2'-bipyrimidine, this is the first system where large differences in the IT energies between isomeric ruthenium-osmium compounds are observed. For all osmium-containing complexes, the extent of electron delocalization is smaller than for the RuRu compound. The most likely explanation is that the orbital overlap between the Ru-bpt orbitals is larger than that for the Os-bpt orbitals. This better orbital overlap also induces the larger splitting of the oxidation potentials observed for the RuRu compound than for the OsOs complex.

Acknowledgment. The authors thank Dr. F. Barigelletti, Dr. L. De Cola, and Prof. Dr. V. Balzani for useful discussions. Furthermore, we thank Unilever Research Laboratories (Vlaardingingen, The Netherlands) for letting us use the electrochemical equipment.

Supplementary Material Available: Tables of atomic fractional coordinates and isotropic thermal parameters of $[(\text{Ru}(\text{bpy})_2)_2(\text{bpt})](\text{CF}_3\text{SO}_3)_3 \cdot 4\text{H}_2\text{O}$, $[(\text{Ru}(\text{bpy})_2)_2(\text{bpt})\text{Os}(\text{bpy})_2](\text{CF}_3\text{SO}_3)_3 \cdot 4\text{H}_2\text{O}$, and the hydrogen atoms of $[(\text{Ru}(\text{bpy})_2)_2(\text{bpt})](\text{CF}_3\text{SO}_3)_3 \cdot 4\text{H}_2\text{O}$, anisotropic thermal parameters of $[(\text{Ru}(\text{bpy})_2)_2(\text{bpt})](\text{CF}_3\text{SO}_3)_3 \cdot 4\text{H}_2\text{O}$, bond distances of $[(\text{Ru}(\text{bpy})_2)_2(\text{bpt})](\text{CF}_3\text{SO}_3)_3 \cdot 4\text{H}_2\text{O}$, bond angles of $[(\text{Ru}(\text{bpy})_2)_2(\text{bpt})](\text{CF}_3\text{SO}_3)_3 \cdot 4\text{H}_2\text{O}$, bond distances of $[(\text{bpy})_2\text{Ru}(\text{bpt})\text{Os}(\text{bpy})_2](\text{CF}_3\text{SO}_3)_3 \cdot 4\text{H}_2\text{O}$, and bond angles of $[(\text{bpy})_2\text{Ru}(\text{bpt})\text{Os}(\text{bpy})_2](\text{CF}_3\text{SO}_3)_3 \cdot 4\text{H}_2\text{O}$ (22 pages); list of structure factors of $[(\text{Ru}(\text{bpy})_2)_2(\text{bpt})](\text{CF}_3\text{SO}_3)_3 \cdot 4\text{H}_2\text{O}$ and $[(\text{bpy})_2\text{Ru}(\text{bpt})\text{Os}(\text{bpy})_2](\text{CF}_3\text{SO}_3)_3 \cdot 4\text{H}_2\text{O}$ (31 pages). Ordering information is given on any current masthead page.